

A general copper-catalysed enantioconvergent radical Michaelis–Becker-type C(*sp*³)–P cross-coupling

Received: 12 July 2022

Accepted: 25 January 2023

Published online: 23 February 2023

 Check for updatesLi-Lei Wang^{1,3}, Huan Zhou^{1,3}, Yu-Xi Cao^{1,3}, Chi Zhang¹, Yang-Qing Ren¹, Zhong-Liang Li², Qiang-Shuai Gu² & Xin-Yuan Liu¹✉

The Michaelis–Becker reaction of H-phosphonates with alkyl halides represents an ideal means for synthesizing alkyl phosphorous compounds. However, the enantioconvergent conversion of racemic alkyl halides into α -chiral alkyl phosphorous compounds in this reaction is an insurmountable challenge because of the inherent S_N2 mechanism. Here we disclose a copper-catalysed enantioconvergent radical Michaelis–Becker-type C(*sp*³)–P cross-coupling. Key to the success of this reaction is the use of multidentate chiral anionic ligands for enhancing the reducing capability of the copper catalyst to favour a stereoablative radical pathway over a stereospecific S_N2-type process. Moreover, the ligand architecture is also able to assist the robust association of copper species with alkyl radicals over H-phosphonates, therefore exerting remarkable chemo- and enantioselectivity. This protocol covers a range of (hetero)benzyl-, propargyl- and α -aminocarbonyl alkyl bromides and chlorides. When allied with follow-up transformations, this method provides a versatile platform for valuable α -chiral alkyl phosphorous building blocks and drug leads.

α -Chiral alkyl phosphorous compounds are important building blocks in organic synthesis and key structural motifs in biologically active molecules, agricultural chemicals and functional materials (Fig. 1a)¹. They are widely utilized as chiral organocatalysts and ligands for asymmetric transformations in organic synthesis^{2–8}. Moreover, phosphonic acids have also been harnessed as potentially interesting acid bioisosteres and are valuable in structure–activity relationship studies in medicinal chemistry^{9–12}. Consequently, the development of catalytic enantioselective methods for constructing chiral C(*sp*³)–P bonds is of paramount importance^{13–28}. The Michaelis–Becker reaction of H-phosphonates with alkyl halides is one of the most efficient approaches for expedited access to C(*sp*³)–P bonds given the ready availability of both starting materials (Fig. 1b)²⁹. Discovered in 1897, it has been used extensively for more than a century together with the related Michaelis–Arbuzov reaction^{30,31}. However, the reaction

has been seldom used in the synthesis of α -chiral alkyl phosphorous compounds because its enantiospecific S_N2 nature^{29,32,33} necessitates the utilization of chiral alkyl halides or the easy epimerization of the alkyl halide racemates. However, earth-abundant 3*d* transition metal catalysis provides a suitable mechanism for enantioconvergence by converting a pair of racemic alkyl halides to the prochiral alkyl radical via a single-electron reduction process, a strategy pioneered by Fu and others^{34–53}. In this context, the development of 3*d*-transition-metal-catalysed enantioconvergent radical Michaelis–Becker-type C(*sp*³)–P cross-coupling would provide a general method toward α -chiral alkyl phosphorous compounds.

As part of our ongoing interest in asymmetric radical reactions^{54–56}, we have found that multidentate chiral anionic ligands can remarkably enhance the reducing capability of Cu(I) catalysts for facile generation of prochiral alkyl radicals from racemic alkyl halides. Accordingly,

¹Shenzhen Grubbs Institute and Department of Chemistry, Guangdong Provincial Key Laboratory of Catalysis, Southern University of Science and Technology, Shenzhen, China. ²Academy for Advanced Interdisciplinary Studies and Department of Chemistry, Southern University of Science and Technology, Shenzhen, China. ³These authors contributed equally: Li-Lei Wang, Huan Zhou, Yu-Xi Cao. ✉e-mail: liuxy3@sustech.edu.cn

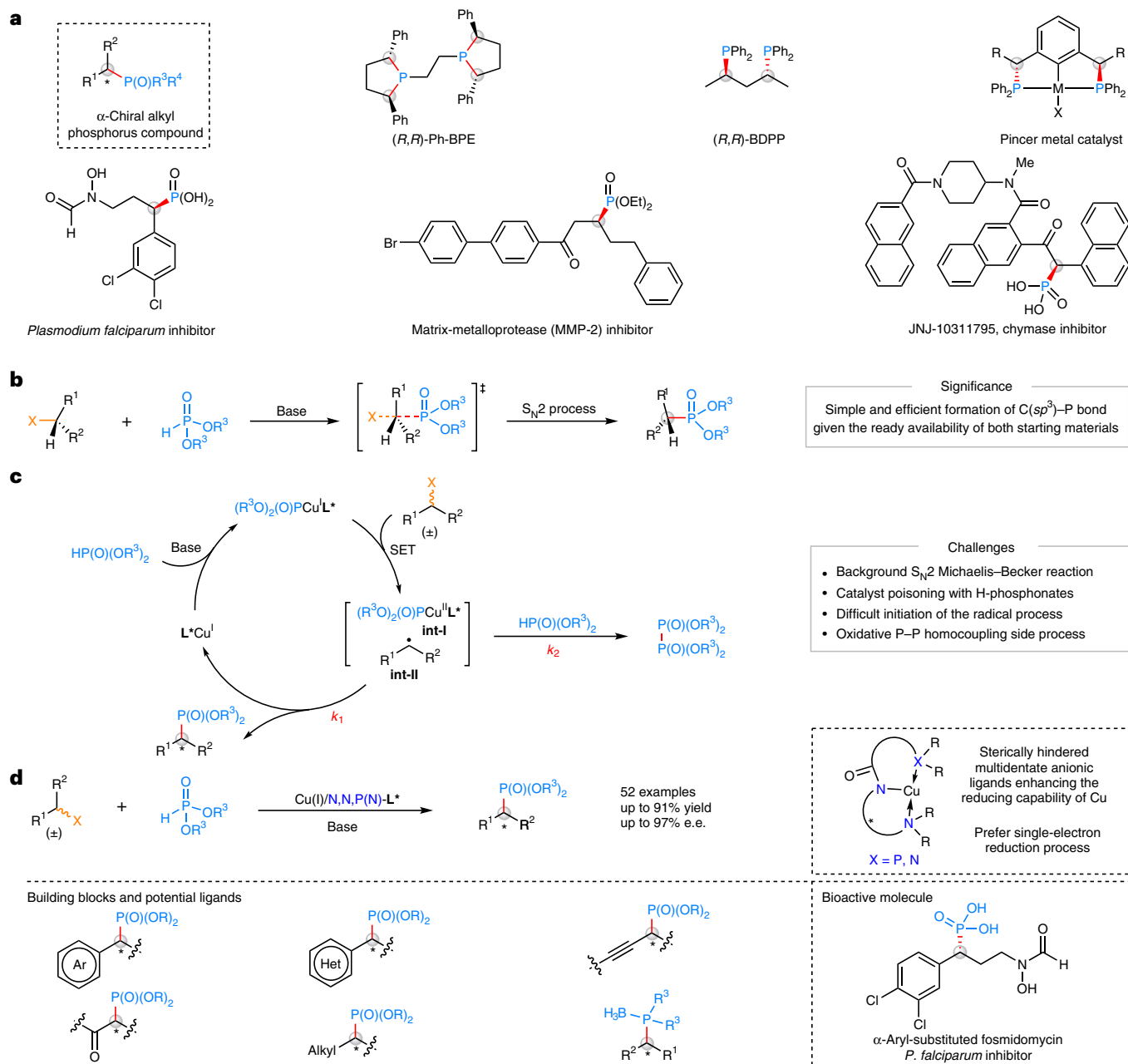


Fig. 1 | Motivation and design of copper-catalysed enantioconvergent radical Michaelis–Becker-type C(sp^3)-P cross-coupling. a, Importance of α -chiral alkyl phosphorus compounds. **b**, Significance of the Michaelis–Becker reaction. **c**, Proposal and challenges for copper-catalysed enantioconvergent radical

C(sp^3)-P coupling. **d**, This work on enantioconvergent radical Michaelis–Becker-type C(sp^3)-P coupling. X, halogen; SET, single-electron transfer; *, chirality; **L***, chiral ligand; Het, heteroarene; BPE, 1,2-bis(phospholano)ethane; BDPP, 2,4-bis(diphenylphosphino)pentane.

a series of enantioconvergent radical C(sp^3)-C/N coupling reactions have been established by our group^{57–62}. Motivated by these exciting precedents, we questioned whether a chiral copper catalyst could realize the enantioconvergent Michaelis–Becker-type C(sp^3)-P cross-coupling. Nonetheless, a number of factors would impede the development of such a process (Fig. 1c): (1) the aforementioned background S_N2 reactions due to the strong nucleophilicity of H-phosphonates; (2) catalyst poisoning and/or chiral ligand displacement with H-phosphonates due to the strong coordination properties^{31,63–67}; (3) the difficult initiation of the radical process due to the weak reducing capability of Cu(I) catalyst; and (4) the easily occurring copper-catalysed oxidative P–P homocoupling (k_2)⁶⁸. Therefore, identifying an appropriate ligand that is capable of selectively promoting the desired enantioconvergent

cross-coupling of CuP(O)(OR³)₂ **int-I** with alkyl radical **int-II** (k_1) amidst other competing processes is important. Here we describe a copper-catalysed enantioconvergent radical Michaelis–Becker-type C(sp^3)-P cross-coupling with remarkable chemo- and enantioselectivities. This reaction covers a range of benzyl-, heterobenzyl-, propargyl- and α -aminocarbonyl alkyl halides and readily available H-phosphonates with high functional group tolerance. It also provides a highly flexible platform to rapidly access diverse synthetically valuable α -chiral alkyl phosphorous building blocks and drug leads when allied with follow-up transformations (Fig. 1d). Given the ready availability of both coupling partners, this strategy would provide an appealing complementary approach to the known methods to synthesize these compounds^{13–28,69–71}.

Table 1 | The effect of different ligands on the model reaction and the optimal results

Reaction scheme: (±)-E1 + P1 $\xrightarrow[\text{Cs}_2\text{CO}_3 \text{ (2.0 equiv.)}, \text{THF, r.t.}]{\text{CuI (15 mol\%), L}^* \text{ (18 mol\%)^a}}$ 1 + 1'

Chemical structures of ligands L*1 through L*14 are shown below the reaction scheme. L*1 and L*2 are N,N-bis(2-aminophenyl)ethane-1,2-diamine derivatives. L*3 is an N,N-bis(2-aminophenyl)ethane-1,2-diamine derivative with a PPh₂ group. L*4 is a P,P-bis(2-aminophenyl)ethane-1,2-diamine derivative with two PPh₂ groups. L*5 is a P,P-bis(2-aminophenyl)ethane-1,2-diamine derivative with a PPh₂ group and a chiral auxiliary. L*6-L*9 are N,N,P-tridentate ligands with various substituents. L*10-L*14 are N,N,P-tridentate ligands with various substituents, including a tert-butyl group in L*14.

Yields and e.e. values for products 1 and 1' are listed for each ligand:

- L*5, Ar = Ph, 1, 16%, 47% e.e.; 1', 11%
- L*6, Ar = 2-MeC₆H₄, 1, trace; 1', trace
- L*7, Ar = 2,6-Me₂C₆H₃, 1, trace; 1', trace
- L*8, Ar = 4-^tBuC₆H₄, 1, 22%, 28% e.e.; 1', 12%
- L*9, Ar = 4-PhC₆H₄, 1, 14%, 30% e.e.; 1', 30%
- L*10, Ar = 3,5-Me₂C₆H₃, 1, 18%, 54% e.e.; 1', 5%
- L*11, Ar = 3,5-(OMe)₂C₆H₃, 1, 30%, 68% e.e.; 1', 17%
- L*12, Ar = 3,5-Ph₂C₆H₃, 1, 27%, 58% e.e.; 1', 9%
- L*13, Ar = 3,5-(ⁱPr)₂C₆H₃, 1, 30%, 40% e.e.; 1', 11%
- L*14, Ar = 3,5-(^tBu)₂C₆H₃, 1, 60%, 81% e.e.; 1', 6% (1, 80%, 90% e.e.; 1', 3%)^b

^aStandard reaction conditions: racemic 1-phenylethyl bromide **E1** (1.5 equiv.), diethyl phosphonate **P1** (0.1 mmol), CuI (15 mol%), ligand (18 mol%) and Cs₂CO₃ (2.0 equiv.) in THF (1 ml) at r.t. for 5 days under argon. Yields were based on ¹H NMR spectroscopic analysis of the crude product using CH₂Br₂ as an internal standard. e.e. values were based on HPLC analysis. ^bThe reaction was conducted at -15 °C for 5 days. The red text indicates the result with the best ligand. ^cBu, *tert*-butyl; ⁱPr, isopropyl.

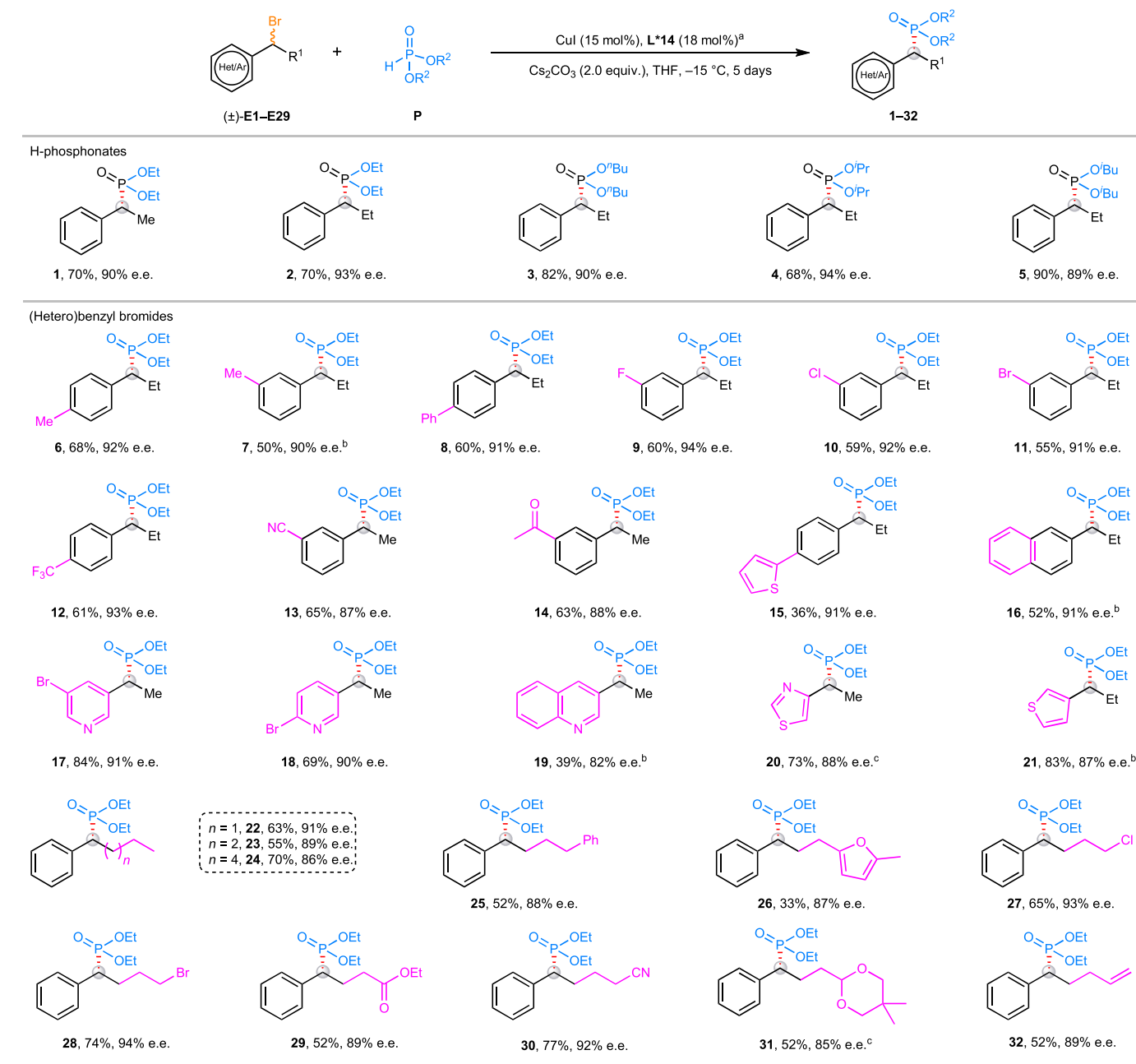
Results and discussion

At the outset, we investigated the reaction of racemic 1-phenylethyl bromide **E1** and diethyl phosphonate **P1** (Table 1). To avoid the S_N2-type Michaelis–Becker background reaction, we first tested the reaction with Cs₂CO₃ in different solvents and found that no strong background reaction was observed in low polar solvents (Supplementary Table 1). To verify the ligand effect in the proposed enantioconvergent radical process, various types of ligands were subsequently screened with CuI as the catalyst in tetrahydrofuran (THF) (Table 1). The bidentate ligands, such as N,N-ligands **L*1** and **L*2**, N,P-ligand **L*3**, and P,P-ligand **L*4**, failed to initiate the single-electron reduction of **E1**. In sharp contrast, Dixon's PPh₃-based cinchona-derived tridentate anionic N,N,P-ligand⁷² **L*5** could initiate this reaction to deliver the desired product **1** in 16% yield with 47% enantiomeric excess (e.e.), along with the P–P homocoupling side product **1'**. Considering the substantial role that the phosphine motif might play in improving reaction efficiency and enantioselectivity, we then screened a series of N,N,P-ligands with different steric and electronic substituents at the P-aryl ring. While *ortho*-substituted N,N,P-ligands **L*6** and **L*7** did not work, *para*-substituted ones **L*8** and **L*9** gave rise to **1** with low chemo- and enantioselectivity. It is noteworthy that 3,5-disubstituted ligands **L*10**–**L*14** showed remarkably good efficiency and enantioselectivity. The N,N,P-ligand **L*14** bearing a steric bulky *tert*-butyl P-substituent gave the best result (60% yield, 81% e.e.) and the P–P homocoupling process could be greatly inhibited (6% yield of **1'**). These results collectively indicated that the use of a sterically bulky N,N,P-ligand is crucial for the robust association of CuP(O)(OR)₂ **int-I** with in-situ-generated alkyl radical **int-II** over H-phosphonate, which would exert effective radical C(sp³)–P coupling while inhibiting oxidative P–P homocoupling (Fig. 1c). After further optimization of reaction parameters, including the copper catalysts, catalyst loading, bases, the molar ratio of the reactants and the reaction temperature (Supplementary Tables 2–6), we identified the optimal conditions as follows: 1.0 equiv. **P1**, 1.5 equiv. **E1**, 15 mol% CuI, 18 mol% **L*14** and 2.0 equiv. Cs₂CO₃ in THF at -15 °C. Under the optimal conditions, the desired product **1** was obtained in 80% yield with 90% e.e. (Table 1).

With the optimized reaction conditions in hand, we examined the generality of the enantioconvergent radical C(sp³)–P coupling reaction (Table 2). With regard to the H-phosphonate scope, a series of H-phosphonate diesters, including diethyl, dibutyl, diisopropyl and diisobutyl groups, can be utilized in this reaction to deliver **1**–**5** in 68–90% yields with 89–94% e.e. However, diphenylphosphine oxide (H(O)PPh₂) is not applicable to the reaction, possibly due to the large steric congestion in the formation of the C(sp³)–P bond with this phosphorus reagent (Supplementary Fig. 1).

We next evaluated the scope of racemic (hetero)benzyl halides using diethyl phosphonate **P1** as a coupling partner. As for the phenyl ring of alkyl bromides, a series of electron-donating and electron-withdrawing substituents at different (*meta* or *para*) positions and bicyclic naphthalene rings were all compatible with the reaction conditions to afford **6**–**16** with 87–94% e.e. Heterobenzyl bromides featuring different types of medicinally relevant heterocycles including pyridine, quinoline, thiazole and thiophene were well accommodated, providing the desired products **17**–**21** in moderate to good yields with excellent enantioselectivity. With respect to the alkyl side chain of benzyl bromides, simple unfunctionalized aliphatic and phenyl groups were suitable for this reaction to access **22**–**25** with good results. More importantly, a gamut of potentially reactive functional groups, such as furan (**26**), primary chloride (**27**) and bromide (**28**), ester (**29**), nitrile (**30**), acetal (**31**) and terminal olefin (**32**) on the side chain of benzyl bromides, were all well tolerated under the reaction conditions. It is noteworthy that excellent chemoselectivity was also observed for the secondary benzyl bromide over primary bromide and chloride (**27** and **28**). The absolute configuration of **1** was determined to be *R* by comparing its HPLC spectrum and optical rotation with those reported in the literature⁷³ and those of other products were assigned in reference to **1**.

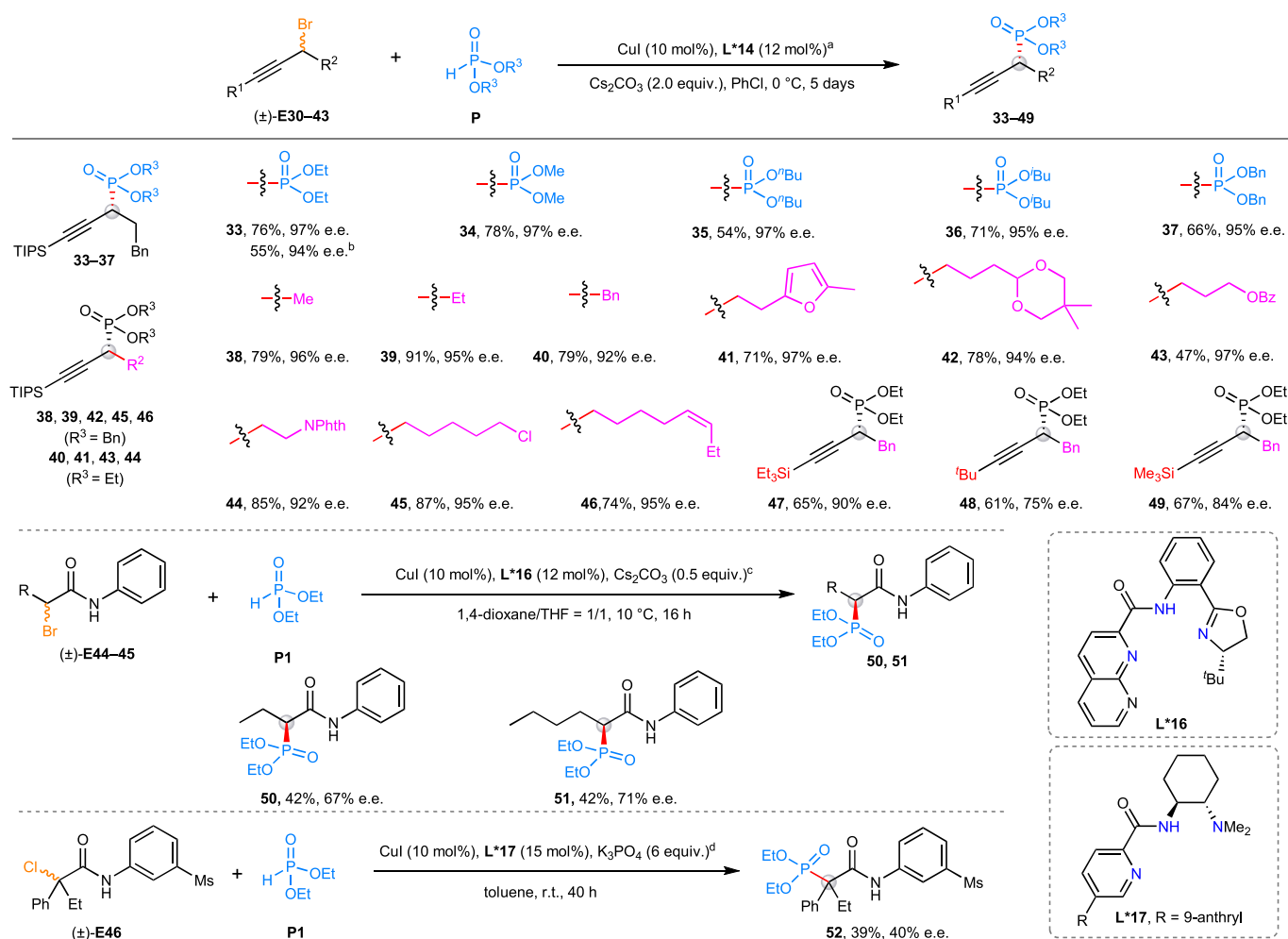
To further explore the generality of this process, more alkyl halides were evaluated (Table 3). Racemic propargyl bromides were first selected as the coupling partner because the easy modification of the alkynyl group renders the corresponding chiral propargyl phosphorous compounds useful as building blocks^{74,75}. As expected, a series of H-phosphonate diesters were successfully coupled with propargyl bromide **E30** to give **33**–**37** in moderate to good yields with excellent enantioselectivity under simply modified reaction conditions (see Supplementary Table 7 for reaction condition optimization). With regard to the propargyl bromide scope, a range of substituents bearing both simple alkyl and functional groups at the aliphatic chain were compatible with the reaction conditions to afford **38**–**46** in 47–91% yields with 92–97% e.e. A gamut of functional groups, such as phenyl ring (**40**), furan (**41**), acetal (**42**), ester (**43**), amide (**44**), primary chloride (**45**) and internal alkene (**46**), were well tolerated under the standard conditions. Additionally, the substrates bearing triethylsilyl (**47**), *tert*-butyl (**48**) and trimethylsilyl (**49**) on the alkynyl moiety were also amenable to the reaction conditions. Further, the less reactive propargyl chloride **E43** was also a suitable substrate for the cross-coupling to provide **33** with slightly low efficiency and similar enantioselectivity. It should be noted that the formation of P–P homocoupling side product **1'** and the slight decomposition of **P1** led to the low yield for substrates that had low reactivities.

Table 2 | Substrate scope for H-phosphonates and (hetero)benzyl bromides

^aStandard reaction conditions: racemic (hetero)benzyl bromide **E1–E29** (1.5 equiv.), H-phosphonate **P** (0.2 mmol), CuI (15 mol%), ligand (18 mol%) and Cs₂CO₃ (2.0 equiv.) in THF (2 ml) at –15 °C for 5 days under argon. Isolated yields are shown. e.e. values were based on HPLC analysis. ^bThe reaction was conducted at –15 °C for 4 days and then at –5 °C for 1 day. ^cThe reaction was conducted at –15 °C for 4 days and then at 0 °C for 1 day. ⁿBu, *n*-Butyl; ⁱBu, isobutyl.

We next investigated the coupling of α -aminocarbonyl alkyl bromides with H-phosphate (Table 3), given the importance of enantioenriched β -carbonylphosphorous compounds as key motifs in potent inhibitors of human mast cell chymase (Fig. 1a)⁷⁶. Nonetheless, α -aminocarbonyl- α -phenyl alkyl bromide **E44** afforded the desired product **50** in poor efficiency and enantioselectivity in the presence of **L*14** or **L*15** (see Supplementary Table 8 for reaction condition optimization), possibly due to the high reactivity of such a substrate. This prompted us to examine less electron-rich N,N,N-ligands and carry out additional systematic optimization of reaction parameters. We identified oxazoline-derived tridentate anionic N,N,N-ligand **L*16** as the best one for the coupling of α -aminocarbonyl alkyl bromides

with good enantioselectivity. In addition, we also tested the reaction of tertiary alkyl chloride **E46** but found that neither **L*14** nor **L*16** gave a good result. We further optimized the reaction conditions of **E46** and identified that N,N,N-ligand (**L*17**) was suitable for the coupling of tertiary alkyl halides⁶² and gave the desired product **52** in 39% yield with 40% e.e. (Table 3 and Supplementary Table 9). These reactions are currently undergoing further optimization in our laboratory. Unfortunately, unactivated alkyl bromides or iodides failed to afford the desired coupling products due to their inertness, and the electrophiles are recovered (Supplementary Fig. 2). Collectively, the broad scope and easy availability of alkyl halides and H-phosphonates enable the coupling reactions to be an important complementary approach to

Table 3 | Substrate scope for propargyl halides and α -carbonyl alkyl halides

^aStandard reaction conditions: racemic **E30-E43** (0.3 mmol), **P** (0.2 mmol), **CuI** (10 mol%), **L*14** (12 mol%) and Cs_2CO_3 (2.0 equiv.) in **PhCl** (2 ml) at 0°C for 5 days under argon. ^bAlkyl chloride **E43** was used and the reaction was conducted at r.t. ^cReaction conditions: racemic **E44** or **E45** (0.2 mmol), **P1** (0.2 mmol), **CuI** (10 mol%), **L*16** (12 mol%) and Cs_2CO_3 (0.5 equiv.) in 1,4-dioxane and THF (2 ml, 1,4-dioxane/THF=1/1) at 10°C for 16 h under argon. ^dReaction conditions: racemic **E46** (0.2 mmol), **P1** (0.3 mmol), **CuI** (10 mol%), **L*17** (15 mol%) and K_3PO_4 (6 equiv.) in toluene at r.t. for 40 h under argon. Isolated yields are shown. e.e. values were based on HPLC analysis. Bn, benzyl; TIPS, triisopropylsilyl; Bz, benzoyl; NPhth, phthalimidyl; Ms, methylsulfonyl.

the reported catalytic methods in the synthesis of α -chiral alkyl phosphorous compounds^{13-28,69-71}.

To demonstrate the synthetic potential of this strategy, facile transformations were performed to convert them to other enantioenriched building blocks (Fig. 2a). For example, we transformed the alkynyl motif of **33** to an alkyl group and obtained **54** through a sequential deprotection and hydrogenation process, which could provide an alternative approach for the $\text{C}(\text{sp}^3)\text{-P}$ cross-coupling of unfunctionalized alkyl halides. In addition, we converted the phosphonate moiety of **2** to chiral phospholane borane **55** using a sequential reduction/alkylation process without remarkable loss of enantiopurity, thereby demonstrating its potential for the synthesis of chiral organocatalysts and ligands. Another interesting application would be the expedient access to a biologically interesting compound (Fig. 2b). Racemic α -aryl-substituted fosmidomycin analogues have shown more favourable physicochemical properties and higher activity than fosmidomycin in inhibiting malaria parasite growth¹¹⁻¹³. However, catalytic asymmetric processes for the synthesis of the enantioenriched substituted fosmidomycin analogues have remained rare⁷⁷⁻⁷⁹. To illustrate this, we evaluated the enantioconvergent $\text{C}(\text{sp}^3)\text{-P}$ coupling of racemic **E47** and dibenzyl phosphonate **P6**, and the reaction delivered the chiral phosphonate **56** in 64% yield with 93% e.e. Then, **56** could be easily

converted into enantioenriched α -3,4-dichlorophenyl-substituted fosmidomycin **58** through a sequential substitution, acylation and deprotection process. Therefore, the present cross-coupling would provide a versatile platform for the diversity-oriented synthesis of such chiral fosmidomycin-derived library and is beneficial to the discovery of promising drug leads.

Concerning the reaction mechanism, a radical trap experiment with 2,2,6,6-tetramethyl-1-piperidinyloxy (TEMPO) revealed that the coupling was completely inhibited and the TEMPO-trapped product **59** was isolated instead (Fig. 2c). Additionally, no apparent enantioenrichment of the recovered alkyl bromide **E5** was observed under typical conditions (Fig. 2d), disfavoring a possible kinetic resolution of **E5**. Moreover, the observed e.e. values of the product remained nearly constant at different time intervals, favouring the involvement of a uniform mechanism throughout the reaction course. These observations strongly support the formation of alkyl radical species from alkyl halides. Overall, all these preliminary experimental results together with previous mechanistic studies⁵⁷⁻⁶² support our initial proposal, as shown in Fig. 1c.

Conclusions

We have established a general copper-catalysed enantioconvergent radical Michaelis–Becker-type $\text{C}(\text{sp}^3)\text{-P}$ cross-coupling of racemic

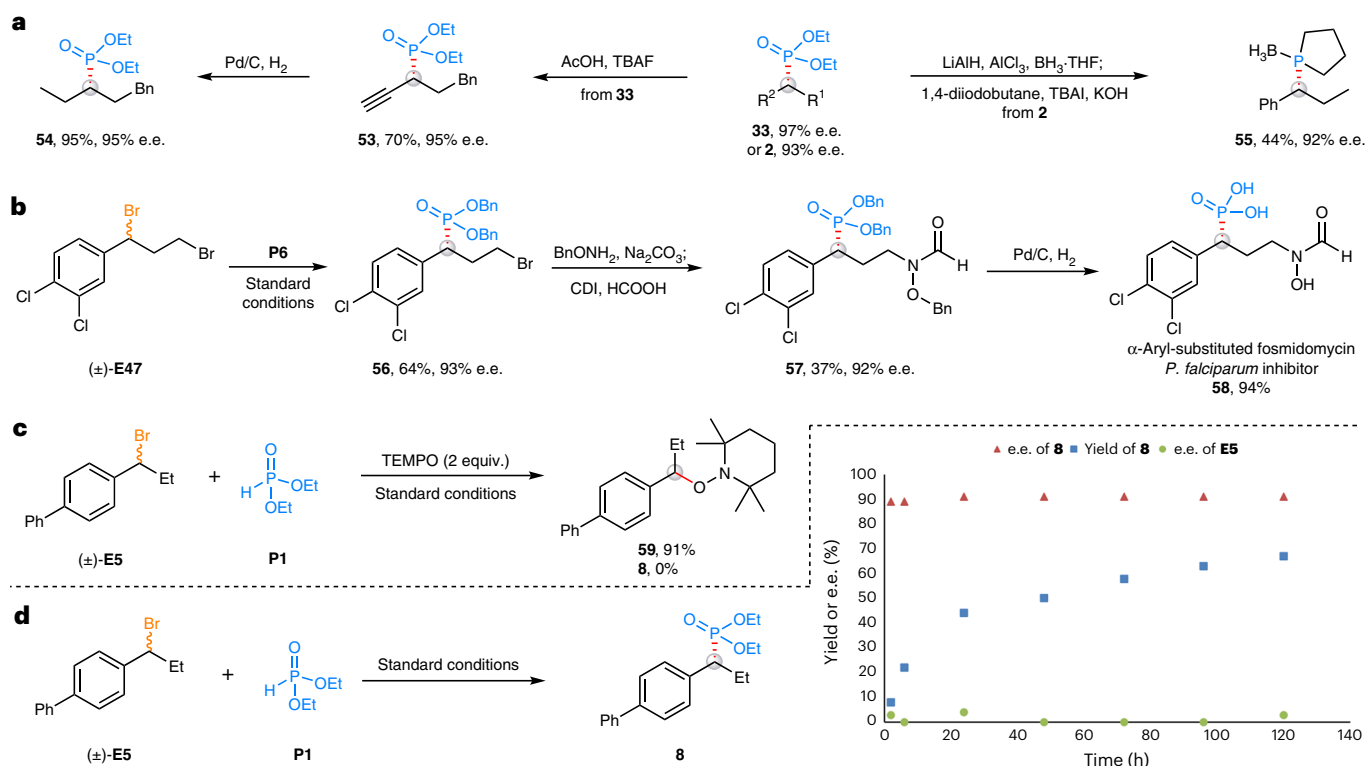


Fig. 2 | Synthetic utility and mechanistic discussion. a, Conversion of enantioenriched products to valuable chiral building blocks. **b**, Expedient synthesis of highly enantioenriched α -3,4-dichlorophenyl-substituted fosmidomycin **58**. **c**, Radical trap experiment with TEMPO. **d**, No apparent

kinetic resolution of the alkyl bromide was observed and the nearly constant product enantiopurity suggested a uniform mechanism during the reaction. TBAF, tetrabutylammonium fluoride; TBAI, tetrabutylammonium iodide; CDI, 1,1'-carbonyldiimidazole.

alkyl halides with H-phosphonates. The key to the success is the use of chiral anionic ligands to forge the robust association of copper species with alkyl radical intermediate over the S_N2 Michaelis–Becker process and P–P homocoupling, therefore exerting radical C(sp^3)–P coupling with excellent chemo- and stereoselectivity. The reaction features a remarkably broad scope for alkyl halides and gives rise to a wide array of α -chiral alkyl phosphorus compounds. The synthetic utility is also demonstrated in the facile transformation of the coupling products to many valuable enantioenriched building blocks and to drug leads. We anticipate that this strategy will open up new avenues for more enantioconvergent carbon–heteroatom cross-coupling reactions of racemic alkyl halides with other heteroatom nucleophiles.

Methods

Synthesis of 1–32

An oven-dried resealable Schlenk tube equipped with a magnetic stir bar was charged with CuI (5.7 mg, 0.03 mmol, 15 mol%), **L*14** (30 mg, 0.036 mmol, 18 mol%) and Cs_2CO_3 (130.0 mg, 0.40 mmol, 2.0 equiv.). The tube was evacuated and backfilled with argon three times. THF (2.0 mL) was then added by syringe under argon. (Hetero)benzyl bromides (0.30 mmol, 1.5 equiv.) and H-phosphonate (0.2 mmol, 1.0 equiv.) were sequentially added into the mixture and the reaction mixture was stirred at -15°C for 5 days. Upon completion, the precipitate was filtered off and washed with ethyl acetate. The filtrate was evaporated and the residue was purified by flash column chromatography on silica gel to afford the desired product.

Synthesis of 33–49

An oven-dried resealable Schlenk tube equipped with a magnetic stir bar was charged with CuI (3.8 mg, 0.020 mmol, 10 mol%), **L*14** (20 mg, 0.024 mmol, 12 mol%) and Cs_2CO_3 (130.0 mg, 0.40 mmol, 2.0 equiv.).

The tube was evacuated and backfilled with argon three times. PhCl (2.0 mL) was then added by syringe under argon. Propargyl halide (0.30 mmol, 1.5 equiv.) and H-phosphonate (0.2 mmol, 1.0 equiv.) were sequentially added into the mixture and the reaction mixture was stirred at 0°C for 5 days. Upon completion, the precipitate was filtered off and washed with ethyl acetate. The filtrate was evaporated and the residue was purified by flash column chromatography on silica gel to afford the desired product.

Synthesis of 50 and 51

An oven-dried resealable Schlenk tube equipped with a magnetic stir bar was charged with CuI (3.8 mg, 0.020 mmol, 10 mol%), **L*16** (9.0 mg, 0.024 mmol, 12 mol%), Cs_2CO_3 (32.6 mg, 0.10 mmol, 0.5 equiv.) and α -carbonyl alkyl halide (0.20 mmol, 1 equiv.). The tube was evacuated and backfilled with argon three times. Mixed solvent of 1,4-dioxane and THF (1/1 vol/vol, 2.0 mL) and H-phosphonate (0.20 mmol, 1.0 equiv.) were then sequentially added into the mixture and the reaction mixture was stirred at 10°C for 16 h. Upon completion, the precipitate was filtered off and washed with ethyl acetate. The filtrate was evaporated and the residue was purified by flash column chromatography on silica gel to afford the desired product.

Synthesis of 52

An oven-dried resealable Schlenk tube equipped with a magnetic stir bar was charged with CuI (3.8 mg, 0.020 mmol, 10 mol%), **L*17** (12.7 mg, 0.03 mmol, 15 mol%), K_3PO_4 (255 mg, 1.2 mmol, 6 equiv.) and α -aminocarbonyl- α -aryl alkyl chloride (0.20 mmol, 1 equiv.). The tube was evacuated and backfilled with argon three times. Toluene and H-phosphonate (0.30 mmol, 1.5 equiv.) were then sequentially added into the mixture and the reaction mixture was stirred at room temperature for 40 h. Upon completion, the precipitate was filtered

off and washed with ethyl acetate. The filtrate was evaporated and the residue was purified by column chromatography on silica gel to afford the desired product.

Data availability

Data relating to the materials and methods, optimization studies, experimental procedures, mechanistic studies, HPLC spectra, NMR spectra and high-resolution mass spectrometry data are available in the Supplementary Information.

References

1. Montchamp, J.-L. (ed.) *Phosphorus Chemistry I: Asymmetric Synthesis and Bioactive Compounds* (Springer, 2015).
2. Tang, W. & Zhang, X. New chiral phosphorus ligands for enantioselective hydrogenation. *Chem. Rev.* **103**, 3029–3069 (2003).
3. Teichert, J. F. & Feringa, B. L. Phosphoramidites: privileged ligands in asymmetric catalysis. *Angew. Chem. Int. Ed.* **49**, 2486–2528 (2010).
4. Xie, J.-H., Zhu, S.-F. & Zhou, Q.-L. Transition metal-catalyzed enantioselective hydrogenation of enamines and imines. *Chem. Rev.* **111**, 1713–1760 (2011).
5. Fernández-Pérez, H., Etayo, P., Panossian, A. & Vidal-Ferran, A. Phosphine–phosphinite and phosphine–phosphite ligands: preparation and applications in asymmetric catalysis. *Chem. Rev.* **111**, 2119–2176 (2011).
6. Ni, H., Chan, W.-L. & Lu, Y. Phosphine-catalyzed asymmetric organic reactions. *Chem. Rev.* **118**, 9344–9411 (2018).
7. Guo, H., Fan, Y. C., Sun, Z., Wu, Y. & Kwon, O. Phosphine organocatalysis. *Chem. Rev.* **118**, 10049–10293 (2018).
8. Xu, G., Senanayake, C. H. & Tang, W. P-chiral phosphorus ligands based on a 2,3-dihydrobenzo[d][1,3]oxaphosphole motif for asymmetric catalysis. *Acc. Chem. Res.* **52**, 1101–1112 (2019).
9. Rodriguez, J. B. & Gallo-Rodriguez, C. The role of the phosphorus atom in drug design. *ChemMedChem* **14**, 190–216 (2019).
10. Kurz, T. et al. Synthesis and antimalarial activity of chain substituted pivaloyloxymethyl ester analogues of fosmidomycin and FR900098. *Bioorg. Med. Chem.* **14**, 5121–5135 (2006).
11. Andaloussi, M. et al. Design, synthesis, and X-ray crystallographic studies of α -aryl substituted fosmidomycin analogues as inhibitors of *Mycobacterium tuberculosis* 1-deoxy-D-xylulose 5-phosphate reductoisomerase. *J. Med. Chem.* **54**, 4964–4976 (2011).
12. Jansson, A. M. et al. DXR inhibition by potent mono- and disubstituted fosmidomycin analogues. *J. Med. Chem.* **56**, 6190–6199 (2013).
13. Glueck, D. S. Catalytic asymmetric synthesis of chiral phosphanes. *Chem. Eur. J.* **14**, 7108–7117 (2008).
14. Albrecht, L., Albrecht, A., Krawczyk, H. & Jørgensen, K. A. Organocatalytic asymmetric synthesis of organophosphorus compounds. *Chem. Eur. J.* **16**, 28–48 (2010).
15. Tappe, F. M. J., Trepohl, V. T. & Oestreich, M. Transition-metal-catalyzed C–P cross-coupling reactions. *Synthesis* **2010**, 3037–3062 (2010).
16. Zhao, D. & Wang, R. Recent developments in metal catalyzed asymmetric addition of phosphorus nucleophiles. *Chem. Soc. Rev.* **41**, 2095–2108 (2012).
17. Feng, J.-J., Chen, X.-F., Shi, M. & Duan, W.-L. Palladium-catalyzed asymmetric addition of diarylphosphines to enones toward the synthesis of chiral phosphines. *J. Am. Chem. Soc.* **132**, 5562–5563 (2010).
18. Nielsen, M., Jacobsen, C. B. & Jørgensen, K. A. Asymmetric organocatalytic electrophilic phosphination. *Angew. Chem. Int. Ed.* **50**, 3211–3214 (2011).
19. Yin, L., Bao, Y., Kumagai, N. & Shibasaki, M. Catalytic asymmetric hydrophosphonylation of ketimines. *J. Am. Chem. Soc.* **135**, 10338–10341 (2013).
20. Nie, S.-Z., Davison, R. T. & Dong, V. M. Enantioselective coupling of dienes and phosphine oxides. *J. Am. Chem. Soc.* **140**, 16450–16454 (2018).
21. Li, Y.-B., Tian, H. & Yin, L. Copper(I)-catalyzed asymmetric 1,4-conjugate hydrophosphination of α,β -unsaturated amides. *J. Am. Chem. Soc.* **142**, 20098–20106 (2020).
22. Yue, W.-J., Xiao, J.-Z., Zhang, S. & Yin, L. Rapid synthesis of chiral 1,2-bisphosphine derivatives through copper(I)-catalyzed asymmetric conjugate hydrophosphination. *Angew. Chem. Int. Ed.* **59**, 7057–7062 (2020).
23. Chen, Y. et al. Asymmetric construction of tertiary/secondary carbon–phosphorus bonds via bifunctional phosphonium salt catalyzed 1,6-addition. *ACS Catal.* **11**, 14168–14180 (2021).
24. Maiti, R. et al. Carbene-catalyzed enantioselective hydrophosphination of α -bromoaldehydes to prepare phosphine-containing chiral molecules. *Angew. Chem. Int. Ed.* **60**, 26616–26621 (2021).
25. Butti, P., Rochat, R., Sadow, A. D. & Togni, A. Palladium-catalyzed enantioselective allylic phosphination. *Angew. Chem. Int. Ed.* **47**, 4878–4881 (2008).
26. Zhang, L., Liu, W. & Zhao, X. Carbon–phosphorus bond formation by enantioselective palladium-catalyzed allylation of diphenylphosphine oxide. *Eur. J. Org. Chem.* **2014**, 6846–6849 (2014).
27. Liu, S., Tanabe, Y., Kuriyama, S., Sakata, K. & Nishibayashi, Y. Ruthenium-catalyzed enantioselective propargylic phosphinylation of propargylic alcohols with phosphine oxides. *Angew. Chem. Int. Ed.* **60**, 11231–11236 (2021).
28. Li, B., Liu, M., Rehman, S. U. & Li, C. Rh-catalyzed regio- and enantioselective allylic phosphinylation. *J. Am. Chem. Soc.* **144**, 2893–2898 (2022).
29. Michaelis, A. & Becker, T. The structure of phosphorous acid. *Chem. Ber.* **30**, 1003–1009 (1897).
30. Bhattacharya, A. K. & Thyagarajan, G. The Michaelis–Arbuzov rearrangement. *Chem. Rev.* **81**, 415–430 (1981).
31. Demmer, C. S., Krogsgaard-Larsen, N. & Bunch, L. Review on modern advances of chemical methods for the introduction of a phosphonic acid group. *Chem. Rev.* **111**, 7981–8006 (2011).
32. Bhat, V., Welin, E. R., Guo, X. & Stoltz, B. M. Advances in stereoconvergent catalysis from 2005 to 2015: transition-metal-mediated stereoablative reactions, dynamic kinetic resolutions, and dynamic kinetic asymmetric transformations. *Chem. Rev.* **117**, 4528–4561 (2017).
33. Zhang, X. & Tan, C.-H. Stereospecific and stereoconvergent nucleophilic substitution reactions at tertiary carbon centers. *Chem* **7**, 1451–1486 (2021).
34. Cherney, A. H., Kadunce, N. T. & Reisman, S. E. Enantioselective and enantiospecific transition-metal-catalyzed cross-coupling reactions of organometallic reagents to construct C–C bonds. *Chem. Rev.* **115**, 9587–9652 (2015).
35. Fu, G. C. Transition-metal catalysis of nucleophilic substitution reactions: a radical alternative to S_N1 and S_N2 processes. *ACS Cent. Sci.* **3**, 692–700 (2017).
36. Choi, J. & Fu, G. C. Transition metal-catalyzed alkyl-alkyl bond formation: Another dimension in cross-coupling chemistry. *Science* **356**, eaaf7230 (2017).
37. Sibi, M. P., Manyem, S. & Zimmerman, J. Enantioselective radical processes. *Chem. Rev.* **103**, 3263–3295 (2003).
38. Nicewicz, D. A. & MacMillan, D. W. C. Merging photoredox catalysis with organocatalysis: the direct asymmetric alkylation of aldehydes. *Science* **322**, 77–80 (2008).

39. Mondal, S. et al. Enantioselective radical reactions using chiral catalysts. *Chem. Rev.* **122**, 5842–5976 (2022).
40. Du, J., Skubi, K. L., Schultz, D. M. & Yoon, T. P. A dual-catalysis approach to enantioselective [2+2] photocycloadditions using visible light. *Science* **344**, 392–396 (2014).
41. Huo, H. et al. Asymmetric photoredox transition-metal catalysis activated by visible light. *Nature* **515**, 100–103 (2014).
42. Hashimoto, T., Kawamata, Y. & Maruoka, K. An organic thiyl radical catalyst for enantioselective cyclization. *Nat. Chem.* **6**, 702–705 (2014).
43. Brimiouille, R., Lenhart, D., Maturi, M. M. & Bach, T. Enantioselective catalysis of photochemical reactions. *Angew. Chem. Int. Ed.* **54**, 3872–3890 (2015).
44. Zhang, W. et al. Enantioselective cyanation of benzylic C–H bonds via copper-catalyzed radical relay. *Science* **353**, 1014–1018 (2016).
45. Murphy, J. J., Bastida, D., Paria, S., Fagnoni, M. & Melchiorre, P. Asymmetric catalytic formation of quaternary carbons by iminium ion trapping of radicals. *Nature* **532**, 218–222 (2016).
46. Kern, N., Plesniak, M. P., McDouall, J. J. W. & Procter, D. J. Enantioselective cyclizations and cyclization cascades of samarium ketyl radicals. *Nat. Chem.* **9**, 1198–1204 (2017).
47. Wang, Y., Wen, X., Cui, X., Wojtas, L. & Zhang, X. P. Asymmetric radical cyclopropanation of alkenes with in situ-generated donor-substituted diazo reagents via Co(II)-based metalloradical catalysis. *J. Am. Chem. Soc.* **139**, 1049–1052 (2017).
48. Wang, F., Chen, P. & Liu, G. Copper-catalyzed radical relay for asymmetric radical transformations. *Acc. Chem. Res.* **51**, 2036–2046 (2018).
49. Proctor, R. S. J., Davis, H. J. & Phipps, R. J. Catalytic enantioselective Minisci-type addition to heteroarenes. *Science* **360**, 419–422 (2018).
50. Biegasiewicz, K. F. et al. Photoexcitation of flavoenzymes enables a stereoselective radical cyclization. *Science* **364**, 1166–1169 (2019).
51. Yang, Y., Cho, I., Qi, X., Liu, P. & Arnold, F. H. An enzymatic platform for the asymmetric amination of primary, secondary and tertiary C(sp³)-H bonds. *Nat. Chem.* **11**, 987–993 (2019).
52. Nakafuku, K. M. et al. Enantioselective radical C–H amination for the synthesis of β-amino alcohols. *Nat. Chem.* **12**, 697–704 (2020).
53. Zhou, Q., Chin, M., Fu, Y., Liu, P. & Yang, Y. Stereodivergent atom-transfer radical cyclization by engineered cytochromes P450. *Science* **374**, 1612–1616 (2021).
54. Zhou, H., Li, Z.-L., Gu, Q.-S. & Liu, X.-Y. Ligand-enabled copper(I)-catalyzed asymmetric radical C(sp³)-C cross-coupling reactions. *ACS Catal.* **11**, 7978–7986 (2021).
55. Gu, Q.-S., Li, Z.-L. & Liu, X.-Y. Copper(I)-catalyzed asymmetric reactions involving radicals. *Acc. Chem. Res.* **53**, 170–181 (2020).
56. Zhang, C., Li, Z.-L., Gu, Q.-S. & Liu, X.-Y. Catalytic enantioselective C(sp³)-H functionalization involving radical intermediates. *Nat. Commun.* **12**, 475 (2021).
57. Dong, X.-Y. et al. A general asymmetric copper-catalysed sonogashira C(sp³)-C(sp) coupling. *Nat. Chem.* **11**, 1158–1166 (2019).
58. Jiang, S.-P. et al. Copper-catalyzed enantioconvergent radical Suzuki-Miyaura C(sp³)-C(sp²) cross-coupling. *J. Am. Chem. Soc.* **142**, 19652–19659 (2020).
59. Su, X.-L. et al. Copper-catalyzed enantioconvergent cross-coupling of racemic alkyl bromides with azole C(sp²)-H bonds. *Angew. Chem. Int. Ed.* **60**, 380–384 (2021).
60. Zhang, Y.-F. et al. Enantioconvergent Cu-catalyzed radical C–N coupling of racemic secondary alkyl halides to access α-chiral primary amines. *J. Am. Chem. Soc.* **143**, 15413–15419 (2021).
61. Wang, P.-F. et al. Design of hemilabile N,N,N-ligands in copper-catalyzed enantioconvergent radical cross-coupling of benzyl/propargyl halides with alkenylboronate esters. *J. Am. Chem. Soc.* **144**, 6442–6452 (2022).
62. Wang, F.-L. et al. Mechanism-based ligand design for copper-catalysed enantioconvergent C(sp³)-C(sp) cross-coupling of tertiary electrophiles with alkynes. *Nat. Chem.* **14**, 949–957 (2022).
63. Kainz, Q. M. et al. Asymmetric copper-catalyzed C–N cross-couplings induced by visible light. *Science* **351**, 681–684 (2016).
64. Chen, C., Peters, J. C. & Fu, G. C. Photoinduced copper-catalysed asymmetric amidation via ligand cooperativity. *Nature* **596**, 250–256 (2021).
65. Lee, H. et al. Investigation of the C–N bond-forming step in a photoinduced, copper-catalyzed enantioconvergent N-alkylation: characterization and application of a stabilized organic radical as a mechanistic probe. *J. Am. Chem. Soc.* **144**, 4114–4123 (2022).
66. Cho, H., Suematsu, H., Oyala, P. H., Peters, J. C. & Fu, G. C. Photoinduced, copper-catalyzed enantioconvergent alkylations of anilines by racemic tertiary electrophiles: synthesis and mechanism. *J. Am. Chem. Soc.* **144**, 4550–4558 (2022).
67. Sutra, P. & Igau, A. Anionic phosph(in)ito ('phosphoryl') ligands: non-classical 'actor' phosphane-type ligands in coordination chemistry. *Coord. Chem. Rev.* **308**, 97–116 (2016).
68. Zhou, Y. et al. Selective P–P and P–O–P bond formations through copper-catalyzed aerobic oxidative dehydrogenative couplings of H-phosphonates. *Angew. Chem. Int. Ed.* **49**, 6852–6855 (2010).
69. Strotman, N. A., Sommer, S. & Fu, G. C. Hiyama reactions of activated and unactivated secondary alkyl halides catalyzed by a nickel/norephedrine complex. *Angew. Chem. Int. Ed.* **46**, 3556–3558 (2007).
70. He, S.-J. et al. Nickel-catalyzed enantioconvergent reductive hydroalkylation of olefins with α-heteroatom phosphorus or sulfur alkyl electrophiles. *J. Am. Chem. Soc.* **142**, 214–221 (2020).
71. Wang, H., Zheng, P., Wu, X., Li, Y. & Xu, T. Modular and facile access to chiral α-aryl phosphates via dual nickel- and photoredox-catalyzed reductive cross-coupling. *J. Am. Chem. Soc.* **144**, 3989–3997 (2022).
72. Sladojevich, F., Trabocchi, A., Guarna, A. & Dixon, D. J. A new family of cinchona-derived amino phosphine precatalysts: application to the highly enantio- and diastereoselective silver-catalyzed isocyanacetate aldol reaction. *J. Am. Chem. Soc.* **133**, 1710–1713 (2011).
73. Wang, D.-Y. et al. Enantioselective synthesis of chiral α-aryl or α-alkyl substituted ethylphosphonates via Rh-catalyzed asymmetric hydrogenation with a P-stereogenic BoPhoz-type ligand. *J. Org. Chem.* **74**, 4408–4410 (2009).
74. Lauder, K., Toscani, A., Scalacci, N. & Castagnolo, D. Synthesis and reactivity of propargylamines in organic chemistry. *Chem. Rev.* **117**, 14091–14200 (2017).
75. Gao, X., Xiao, Y.-L., Zhang, S., Wu, J. & Zhang, X. Copper-catalyzed enantioselective trifluoromethylthiolation of secondary propargyl sulfonates. *CCS Chem* **2**, 1463–1471 (2020).
76. Greco, M. N. et al. Discovery of potent, selective, orally active, nonpeptide inhibitors of human mast cell chymase. *J. Med. Chem.* **50**, 1727–1730 (2007).
77. Maerten, E., Cabrera, S., Kjaergaard, A. & Jørgensen, K. A. Organocatalytic asymmetric direct phosphorylation of α,β-unsaturated aldehydes: mechanism, scope, and application in synthesis. *J. Org. Chem.* **72**, 8893–8903 (2007).
78. Cheruku, P., Paptchikhine, A., Church, T. L. & Andersson, P. G. Iridium-N,P-ligand-catalyzed enantioselective hydrogenation of diphenylvinylphosphine oxides and vinylphosphonates. *J. Am. Chem. Soc.* **131**, 8285–8289 (2009).
79. Dong, K., Wang, Z. & Ding, K. Rh(I)-catalyzed enantioselective hydrogenation of α-substituted ethenylphosphonic acids. *J. Am. Chem. Soc.* **134**, 12474–12477 (2012).

Acknowledgements

We thank the National Key R&D Program of China (2021YFF0701604 and 2021YFF0701704, X.-Y.L.), the National Natural Science Foundation of China (22025103 and 21831002, X.-Y.L.), the Guangdong Innovative Program (2019BT02Y335, X.-Y.L.), the Guangdong Provincial Key Laboratory of Catalysis (2020B121201002, X.-Y.L.), the Shenzhen Science and Technology Program (KQTD20210811090112004, X.-Y.L.) and Shenzhen Special Funds (JCYJ20200109141001789, X.-Y.L.) for financial support. We thank the SUSTech Core Research Facilities for assistance with compound characterization.

Author contributions

X.-Y.L. conceived and supervised the project. L.-L.W., H.Z., Y.-X.C., C.Z., Y.-Q.R., Z.-L.L. and Q.-S.G. designed and performed the experiments and analysed the data. X.-Y.L., and L.-L.W. wrote the paper. All authors discussed the results and commented on the manuscript.

Competing interests

The authors declare no competing interests.

Additional information

Supplementary information The online version contains supplementary material available at <https://doi.org/10.1038/s44160-023-00252-3>.

Correspondence and requests for materials should be addressed to Xin-Yuan Liu.

Peer review information *Nature Synthesis* thanks Wei-Liang Duan, Choon-Hong Tan and the other, anonymous, reviewer(s) for their contribution to the peer review of this work. Primary handling editor: Peter Seavill, in collaboration with the *Nature Synthesis* team.

Reprints and permissions information is available at www.nature.com/reprints.

Publisher's note Springer Nature remains neutral with regard to jurisdictional claims in published maps and institutional affiliations.

Springer Nature or its licensor (e.g. a society or other partner) holds exclusive rights to this article under a publishing agreement with the author(s) or other rightsholder(s); author self-archiving of the accepted manuscript version of this article is solely governed by the terms of such publishing agreement and applicable law.

© The Author(s), under exclusive licence to Springer Nature Limited 2023